Traveling Magnetic Field Plasma Accelerator

IEPC-2013-86

Presented at the 33^{rd} *International Electric Propulsion Conference,*
The George Washington University, Washington, D.C., USA
October 6–10, 2013

Andrea Lucca Fabris*
University of Padova, Padova, 35131, Italy

Mark A. Cappelli†
Stanford University, Stanford, CA 94305, USA

This paper describes a new dual-stage propulsion system based on a traveling magnetic field accelerator. The plasma produced in a primary ionization source is injected into the second stage where it is accelerated by means of a traveling magnetic field. An analysis through a particle-in-cell model highlights the role of electrons as carriers of the acceleration: the magnetic field directly acts on electrons creating a space charge at the magnetic front, where the resulting electric field also accelerates the ions.
A prototype of the system has been built using a transmission line configuration for a preliminary experimental investigation. A microwave source is used as the primary ionization stage. The experimental setup includes current probes, magnetic field probes and time-of-flight probes.

Nomenclature

I_{sp}	= specific impulse
PIT	= Pulsed Inductive Thruster
$FARAD$	= Faraday Acceleration with Radio Frequency Assisted Discharge
ECR	= electrons cyclotron resonance
PIC	= particle-in-cell
v_t	= propagation velocity of the traveling magnetic field
w	= magnetic pulse width
τ_{ci}	= ion cyclotron period
τ_{ce}	= electron cyclotron period

I. Introduction

Electrodeless propulsion can be considered to be the next step in the technological evolution of space propulsion, since it is able to overcome some critical issues of consolidated propulsion systems, particularly the erosion of electrodes and of the plasma channel wall. Acceleration grid erosion is a lifetime-limiting process in ion thrusters as is wall and cathode erosion in Hall thrusters[1]. The absence of the external neutralizer is an attractive advantage that is offered by electrodeless propulsion systems. In the last decades several research efforts have been dedicated to the development of new electrodeless propulsion concepts. Helicon thrusters[2] are a promising technology, and research on helicon double-layer thrusters, exploring different working regimes and performance, is ongoing in Australia, USA, Europe and Japan. Other more unconventional solutions have been proposed in the last few years, such as ion acceleration with beating

*PhD Candidate, Center of Studies and Activities for Space, andrea.luccafabris@gmail.com.
†Professor, Mechanical Engineering Department, Thermosciences group, cap@stanford.edu.

electrostatic waves[3] or plasma acceleration produced by a rotating electric field[4]. Another electrodeless system is the pulsed inductive thruster (PIT)[5]. In this device a strong current is pulsed through a flat coil discharging a bank of capacitors. The effect is a strong azimuthal field which breaks down the neutral gas and gives rise to an azimuthal current in the opposite direction relative to that flowing through the coil. The azimuthal current interacts with the radial component of the magnetic field giving an axial thrust component. Efficiencies up to 50% and I_{sp} up to $2240s$ have been achieved for $4kJ$ energy pulses. An evolution of this concept is represented by the FARAD (Faraday Acceleration with Radio Frequency Assisted Discharge)[6] thruster developed at Princeton University which consists of a double stage system with: 1) a helicon discharge for primary ionization, 2) an inductive flat coil for plasma acceleration, relying on the same principle as that of the PIT. In the PIT the strong azimuthal field both ionizes and accelerates the propellant, whereas in the FARAD these two stages take place separately (partially, since the azimuthal field provides an additional ionization). As a result, accelerated current sheets form at lower pulse energies (down to $44J$). A sheet velocity of $12000m/s$ has been measured for a $78.5J$ pulse.

In this paper an alternative plasma acceleration concept is proposed, based on a axially-propagating magnetic field. The accelerator is intended to be used as an acceleration stage in a multi-stage thruster. During the 1960s and 1970s several studies[7−15] were carried out on plasma acceleration by means of propagating magnetic fields. In the most typical configuration, the plasma is injected in a cylindrical dielectric tube surrounded by an array of coaxial coils with currents progressively phase-shifted according to the target propagation velocity of the magnetic field, usually within the range $10^4 - 10^5 m/s$. The magnetic field acts as a piston pushing the plasma downstream and accelerating it at velocities close to the traveling velocity of the fields. Both theoretical analysis and experimental tests were performed demonstrating the viability and effectiveness of the concepts. Propagating fields with various configurations (flat, mirror shaped, cusped shaped) were tested and the effect of an additional magnetostatic background field was also investigated[11]. Typically, the coils are powered by polyphase networks[8,9,12,14] or are integrated into a transmission line circuit[7,15]. The operating mode can be pulsed[11,15] or with continuous power application[7−10,12,14]. The traveling velocity can be varied along the acceleration direction by tuning the values of the circuit elements. For instance, Haldeman's system[7] presents a linear increase of the phase velocity of the propagating field (from 4000 to $12000m/s$) along the acceleration channel in order to optimize the energy transferred to the gas flow per unit length. The system consists of a sequence of coils with currents progressively phase-shifted and operated in continuous power mode at $30kHz$. The chosen circuit scheme is a slow transmission line operating in ring mode. In a transmission line the wave travels with a velocity depending on the inductance and capacitance per unit length. Thus the phase velocity can be varied regulating those parameters along the accelerator. The experimental results along with a mathematical model demonstrate the feasibility of coupling the plasma to the traveling magnetic field giving an acceleration effect.

The effect of an additional background field on the overall plasma acceleration is explored by Light[11], focusing particularly on its magnitude and its direction (parallel or antiparallel relative to the acceleration direction). This uniform axial magnetic field affects the shape of the "magnetic piston" and enhances the plasma confinement from the accelerator walls. Light's system is operated in pulsed mode ($2.5kJ/pulse$), discharging a bank of capacitors on a transmission line network with a constant propagation velocity to produce a field traveling at $1.1 \cdot 10^5 m/s$. The magnetic piston has a strength of $6000G$ and the additional field has a magnitude of up to $4000G$. The position of the magnetic piston is monitored through radial B-field probes and the position of the pushed plasma is detected by means of photomultiplier tubes along the acceleration channel. The experiments demonstrate that the magnetic piston is effectively accelerating the plasma and the velocity of the plasma increases with the strength of the static background field both in the parallel and antiparallel configuration.

A research program aimed at the development of a traveling magnetic wave plasma engine was carried out at NASA Lewis Research Center[8−10]. Experiments with both four and ten-coil configurations were performed. The velocity of the magnetic wave is $46500m/s$ in both cases. The power for the coils is supplied by two $13kW$ generators operating at $150kHz$. A pendulum momentum probe is placed at the exhaust of the accelerator to provide an estimation of the thrust. The operating propellants are xenon and argon with mass flow rates within the range $0.2 - 2.6 \cdot 10^{-6} kg/s$ and input power of $1 - 5kW$. The axial magnetic field strength on the axis is about $70 - 80G$. The measured thrust spans from 0.8 up to $2.5 \cdot 10^{-2} N$. For the four-coil configuration, a propulsive efficiency of 0.1 and a specific impulse of $3200s$ are measured for argon and 0.23 and 4200s for xenon, respectively. The effect of a coaxial ferrite core is also investigated in an attempt to increase the the strength of the radial component of the magnetic field. However, the overall effect is negative because of the drag and heat losses due to the core.

An alternative configuration is proposed by Heflinger[14], characterized by a rectangular duct with a transverse geometry of the magnetic field which is perpendicular to the traveling direction. The magnetic field has an intensity of about $500G$, travels with a velocity of $54000m/s$, and is generated by four coils powered at $480kHz$. The neutral gas is ionized by the electric field associated with the propagating magnetic field. Several propellants are tested. The best performance is obtained with helium, showing a specific impulse up to $6000s$ and an efficiency of about 0.5 for a power of $160kW$ and a mass flow of $5 \cdot 10^{-5}kg/s$.

Despite the significant prior history and promising results of these traveling wave concepts, the system described here is still in a proof-of-concept phase. Particularly, its application to space propulsion in the low power range ($< 250W$) has never been explored. In this paper we present the results of our preliminary studies on this traveling magnetic field plasma accelerator, focusing on the understanding of the basic physics of the device through both analytical and numerical simulations of the plasma acceleration process. Along with the simulations, we have designed a system of coils able to produce a magnetic field traveling with a velocity of about $20000m/s$. The system is based on a transmission line scheme operating either in continuous power mode, employing a $300W - 280kHz$ generator, or in pulsed mode in the range $0.7 - 5J/pulse$. The mass flow rate range we intend to explore is $1 - 5 \cdot 10^{-7}kg/s$. Preliminary operation of this design includes a neon plasma source driven by an Evanson microwave cavity[16] operating at $2.45GHz$ as primary ionization stage.

The paper is structured as follow: a basic description of a propulsion system based on a traveling magnetic field accelerator is provided in section II; 1-D particle-in-cell code simulations aimed to provide physical insight of the acceleration mechanism are described in section III ; the preliminary experiment set up to characterize the accelerator's operation is illustrated in section IV.

II. Thruster concept

The thruster consists of two-stages:

- a plasma source stage to ionize the neutral propellant flow;
- a plasma accelerator which exploits a traveling magnetic field to accelerate and eject the plasma, generating thrust.

Different types of plasma sources can be employed as a first stage. Due to the high efficiency a helicon source is the best candidate as used in the FARAD concept[6]. An alternative solution is a microwave discharge operating in the ECR mode.

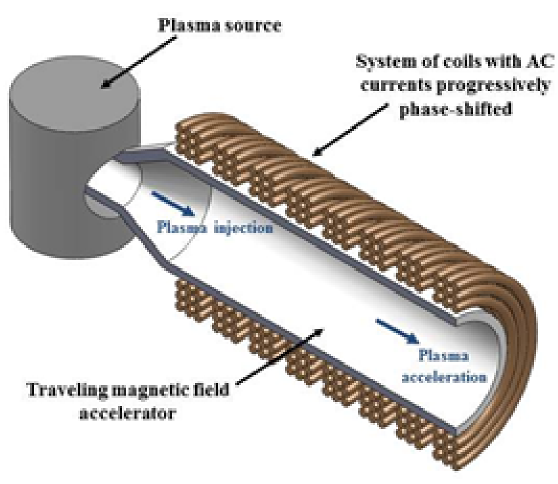

Figure 1. Propulsion system schematic.

The plasma produced in the source stage is injected into the acceleration channel, which consists of a cylindrical quartz tube. A sequence of coaxial coils with currents progressively phase-shifted or delayed is located around the tube in order to generate the traveling field. According to Faraday's law, an azimuthal electric field is associated to the time-varying magnetic field, generating an azimuthal current in the plasma (Ohm's law)[13].

$$\nabla \times \mathbf{E} = -\frac{\partial \mathbf{B}}{\partial \mathbf{t}} \tag{1}$$

$$\mathbf{J} = \sigma \mathbf{E} \tag{2}$$

This azimuthal current interacts with the radial component of the magnetic field giving a force term in the axial direction.

$$\mathbf{f} = \mathbf{J} \times \mathbf{B} \tag{3}$$

Among the different configurations of circuits able to produce a traveling magnetic field, we have selected a matched transmission line. The coils of the accelerator constitute the inductors of the transmission line. Capacitors are connected in parallel in the junctions between the inductors. The velocity of a wave propagating along a transmission line (considered lossless in this preliminary description) depends on the inductance l and capacitance c per unit length. The velocity of the traveling wave can be imposed selecting the proper values of l and c.

$$v_t = \frac{1}{\sqrt{lc}} \tag{4}$$

The transmission line can be closed by a resistive load equal to its intrinsic load $Z_0 = \sqrt{l/c}$ or operated in a ring configuration[7]. Moreover the mode of operation can be either continuous or pulsed. In the former case a Radio-Frequency power supply is used, the currents in the coils are sinusoidal and progressively phase-shifted, as illustrated in Fig. 3. In the pulsed mode a capacitor is discharged to produce a current pulse traveling along the line. The current peak in each coil is delayed relative to the previous one according to the wave speed.

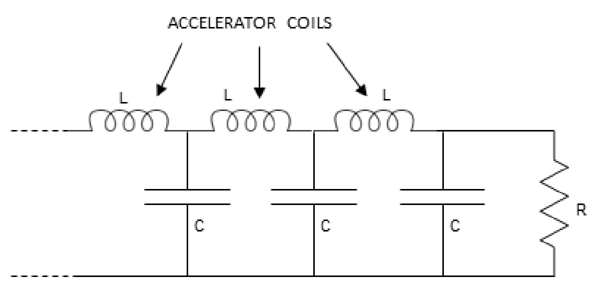

Figure 2. Transmission line.

The shape of the magnetic field generated by the transmission line strongly depends on the mode of operation, continuous or pulsed. The field on a longitudinal plane (r, z) of the accelerator at a given time can be estimated exploiting the magnetostatic approximation, based on the instantaneous currents flowing in each coil at the considered time. An example of a traveling magnetic field pattern produced by a transmission line powered by an RF power supply is depicted in Fig. 4. The field presents radial cusped-shaped regions alternating with regions in which the field is mainly axial. The field direction (both of the radial and axial component) changes along the accelerator, however the induced electric field and the associated plasma azimuthal current also reverse, giving an axial force component that always points downstream.

In contrast, the field generated by a current pulse (Fig. 5) has a simple mirror shape and does not present inversions along the accelerator. The magnetic field propagates along the accelerator and acts as a piston on the plasma.

As mentioned in the introduction, the system we designed is able to produce a propagating magnetic field with an estimated traveling velocity of $21500m/s$. The transmission line can be either continuously powered by a $280kHz - 300W$ RF generator or operated in a pulsed mode discharging a $1\mu F$ capacitor giving energy pulses in the range $0.7 - 5J$. The channel of the accelerator is made of a quartz tube with a diameter of $25mm$. The tube narrows on the plasma injection side to house the Evanson microwave cavity[16] used as a primary ionization stage. The microwave source operates at $2.45GHz$ with a power of $50 - 100W$. The input

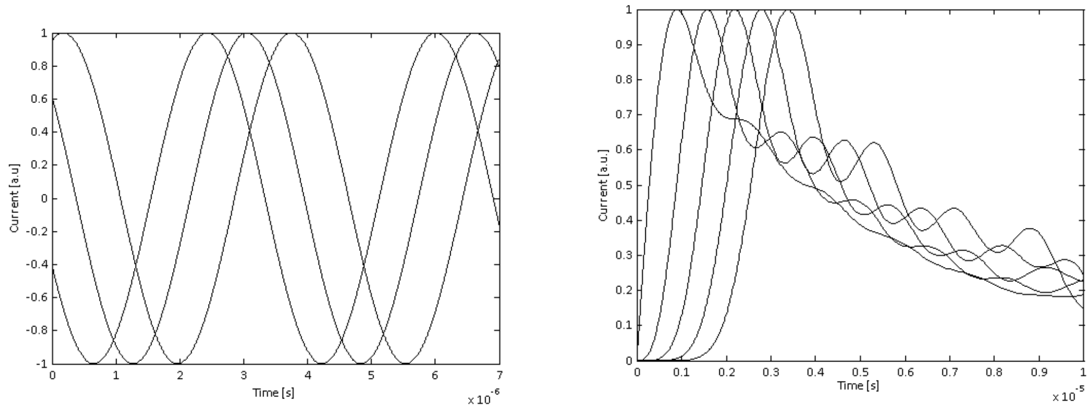

Figure 3. On the right: currents in three consecutive coils of a transmission line powered through a $280kHz$ RF generator. On the left: current pulse propagating through five consecutive coils.

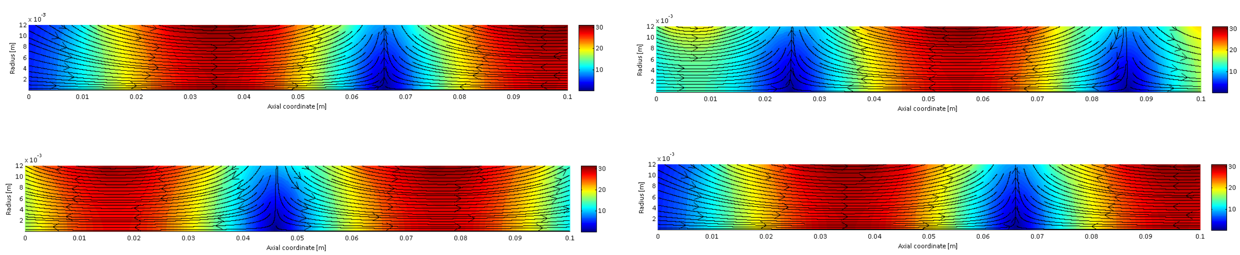

Figure 4. Example of magnetic field (in [G]) generated by a current pulse propagating along a transmission line at different time frames: $1, 3, 5, 7\mu s$. The propagation velocity is $22500m/s$.

mass flow rate range is $1 - 5 \cdot 10^{-7} kg/s$ of argon. We would like to explore also the use of lighter propellants such as helium and neon.

III. 1D Particle-In-Cell simulations

A preliminary investigation of the physical acceleration mechanism has been performed through a 1-D particle-in-cell code with both kinetic ions and electrons. The aim is to highlight possible physical mechanisms caused by the different dynamics of the two species when forced by a magnetic pulse. We believe that only electrons are directly affected by the traveling field for the strength and velocity ranges considered, due to their higher mobility. On the other hand the direct effect of the magnetic field on ion motion is negligible since $\tau_{ci} >> w/2v_t$, where τ_{ci} is the ion cyclotron period, w is the magnetic pulse spatial width and v_t is its propagation velocity. The different dynamics of the two species create a charge separation and a consequent electric field which accelerates ions. A similar consideration has been pointed out by Jones[9]. The fully kinetic PIC code simulates the ion and electron motion and solves self-consistently the electric field arising from the local charge distribution, and therefore is a good candidate to highlight this effect.

A. Code overview.

The code is based on a 1-D electrostatic particle-in-cell model for the simulation of plasmas[17]. In the code the plasma behavior is described using a particle approach both for ions and electrons. Physical particles are aggregated in computational particles in order to reduce the computational effort. A macroparticle is treated as a single particle but owns the extensive properties of the group of particles it represents, i.e. mass and charge for the peculiar case. Macroparticles move in a continuum space, in this case one-dimensional, forced by the electric and magnetic fields. The fields are instead calculated in the nodes of a discrete grid. The cell dimension is a parameter correlated to the specific simulated plasma. The macroparticles motion

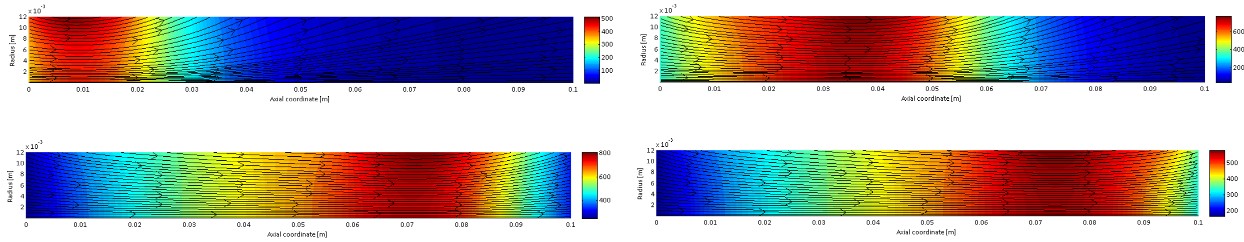

Figure 5. Example of magnetic field (in [G]) generated by a current pulse propagating along a transmission line at different time frames: $1, 3, 5, 7\mu s$. The propagation velocity is $17500 m/s$.

obeys to the Newton-Lorentz equations and the force acting on them is computed by interpolating the fields between the closest grid points. The effect of magnetic gradients on particles motion is included through the force term $-\mu\nabla B$ along the considered dimension, where μ is the magnetic moment defined as:

$$\mu = \frac{mv_\perp^2}{2B} \tag{5}$$

In the last equation $v_\perp$ is the velocity component perpendicular to the field lines. In the simulations presented here we assume magnetized electrons and non-magnetized ions since only electrons are mobile enough to dynamically respond to the traveling magnetic pulse. We consider the magnetic moment of electrons a good adiabatic invariant, since the rate of change of the magnetic field is much slower than the electrons cyclotron period $w/2v_t >> \tau_{ce}$. The introduction of the magnetic moment and the assumption of its conservation allows to take into account the shape of the magnetic field, in particular the axial variation of its intensity. With these assumptions the ion and electron equations of motion become:

$$m_e \frac{dv_{ze}}{dt} = -e\frac{d\phi}{dz} - \mu\frac{dB}{dz} \tag{6}$$

$$m_i \frac{dv_{zi}}{dt} = e\frac{d\phi}{dz} \tag{7}$$

The equations of motion are integrated through a leapfrog algorithm, where the location of the particle is evaluated at whole time steps, whereas the velocity is offset by half a time step:

$$v_z^{(n+1/2)} = v_z^{(n-1/2)} + \frac{F(z^{(n)})}{m}\Delta t \tag{8}$$

$$z^{(n+1)} = z^{(n)} + v_z^{(n+1/2)}\Delta t \tag{9}$$

The electric field is expressed as the gradient of the potential $E_z = -d\phi/dz$, while the potential is related to the charge density by the Poisson equation.

$$\frac{d^2\phi}{dz^2} = -\frac{\rho}{\epsilon_0} \tag{10}$$

The Poisson equation is solved at the nodes of the grid using a central finite difference method:

$$\frac{\phi_{j-1} - 2\phi_j + \phi_{j+1}}{dz^2} = -\frac{\rho_j}{\epsilon_0} \tag{11}$$

The boundary conditions at the edges of the simulation domain are Dirichlet type. The electric field is calculated from the potential applying a five point stencil method:

$$E_j = -\frac{-\phi_{j+2} + 8\phi_{j+1} - 8\phi_{j-1} + \phi_{j-2}}{12\Delta x} \tag{12}$$

The force is interpolated linearly to the particle location from the adjacent cell boundaries. Similarly, the charge density is calculated on the grid knowing the number of particles in the adjacent cells and weighting their contributions depending on their distance from the grid nodes. The particles are initially loaded in a random position of the simulation domain according to a uniform spatial distribution and with a random velocity according to an overall Maxwellian population. The plasma is considered initially quasi-neutral, so ion-electron pairs are loaded in the same position. The overall computational scheme is reported in Fig. 6.

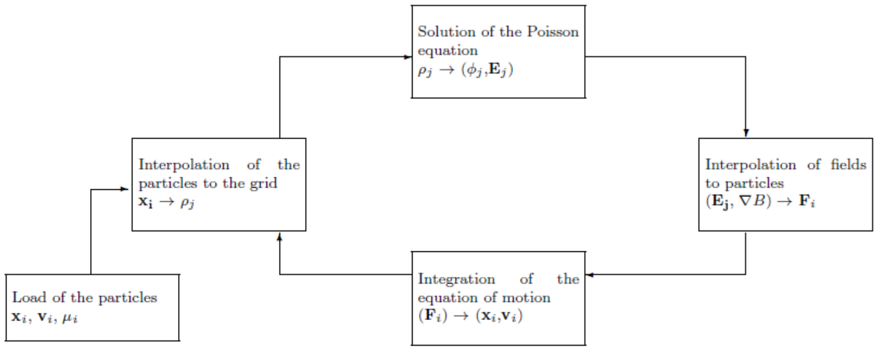

Figure 6. PIC code basic scheme.

B. Traveling magnetic field simulation.

The numerical domain consists of a $2.5cm$-diameter $10cm$-length plasma cylinder in which a Gaussian-shaped magnetic pulse propagates with a traveling velocity of $30000m/s$. The pulse intensity is $400G$ and its width $6mm$. A fully ionized collisionless plasma consisting of two species (ions and electrons) is simulated. The electron temperature is set to $4eV$ and the ion temperature to $0.1eV$. The unperturbed plasma density is $6 \cdot 10^{13} m^{-3}$. The ion species consists of hydrogen ions. The weight of a numerical macroparticle is 20000, i.e. 20000 physical particles are aggregated in a numerical macroparticle. For each ion crossing a boundary a new ion-electron pair is loaded in the domain. The overall number of simulated particles is 120000, giving an average number of particles per cell equal to 400. The cells dimension spatially resolves the Debye length with $\lambda_D/\Delta x \approx 3$. The time step has been chosen to satisfy the conditions required by particle-in-cell codes, i.e. the solution of characteristic plasma frequencies. For the aforementioned parameters the plasma period is $14.4ns$, the ion cyclotron period is $1.64\mu s$, the electron cyclotron period is $0.9ns$ (considering the peak magnetic field), whereas the time scale of the magnetic pulse is $0.1\mu s$. Both the boundaries are represented with a Dirichlet type condition, imposing a null voltage.

The simulation is run for about $10\mu s$ in order to allow the sheath formation at the boundaries and to reach a steady unperturbed condition. Subfigures 7-12,a) represent the plasma properties before the action of the traveling magnetic field. In the central region the plasma is macroscopically quasi-neutral, whereas in the regions close to the boundaries a positive net charge takes place, due to the higher ion density in comparison to the electron density. Moreover, in the sheaths the ions are accelerated above the Bohm velocity satisfying the Bohm criterion. The potential in the bulk plasma relative to the wall is about $13V$ in good agreement with that calculated through the analytical formula[18]:

$$\Delta\phi = \frac{K_B T_e}{2e}\left[1 + \ln\left(\frac{M_i}{2\pi m_e}\right)\right] \tag{13}$$

At $10\mu s$ the traveling magnetic field is launched and travels through the plasma from the left edge to the right edge of the domain. In all the figures below the position of the field is reported in order to give a reference during its motion.

Figures 7 and 8 illustrate the electron and ion phase spaces at different time steps. The propagating magnetic field locally affects both the ion and electron velocity distribution functions even if through different driver mechanisms. As the field runs through the plasma it pushes electrons downstream whereas ions are initially unperturbed since the time scale of their kinetic response is slower. As a consequence, a charge separation forms at the moving front of the magnetic field, with an electron rich region followed by an ion rich region (see Fig. 9), i.e., a double layer formation.

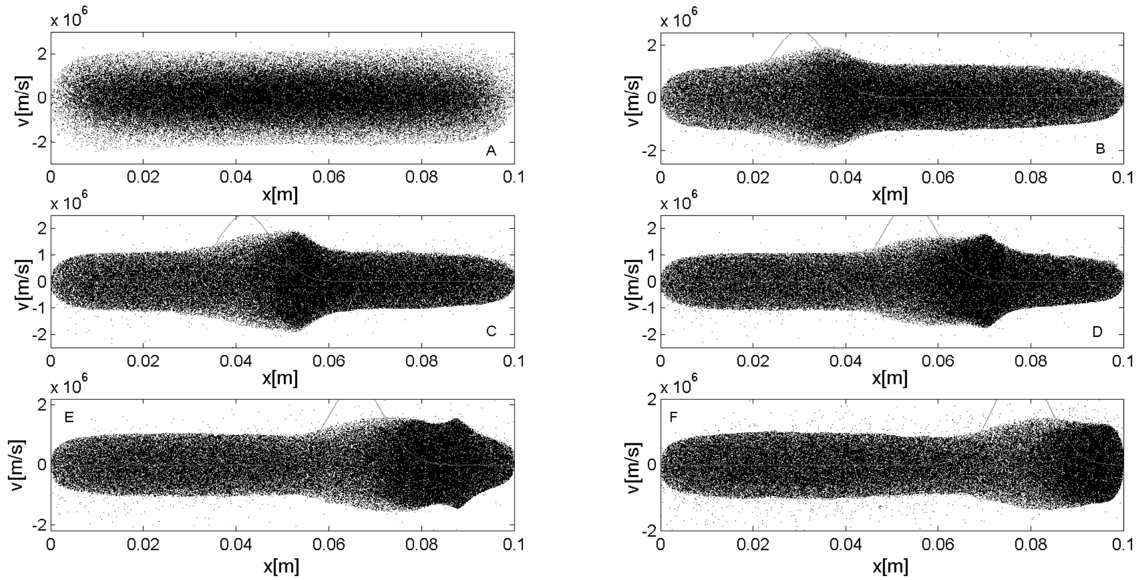

Figure 7. Electron phase space at different time steps. A: $10\mu s$. **B:** $11\mu s$. **C:** $11.4\mu s$. **D:** $11.8\mu s$. **E:** $12.2\mu s$. **F:** $12.6\mu s$.

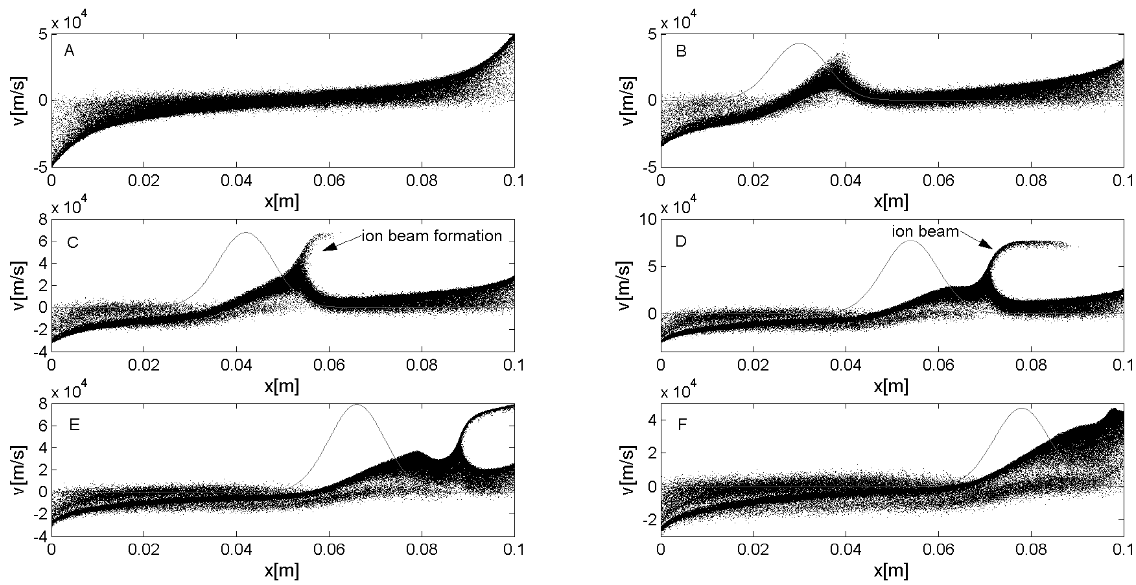

Figure 8. Ion phase space at different time steps. A: $10\mu s$. **B:** $11\mu s$. **C:** $11.4\mu s$. **D:** $11.8\mu s$. **E:** $12.2\mu s$. **F:** $12.6\mu s$.

Since the net charge is no longer null a potential hill and associated electric field arise, holding electrons and accelerating ions. The ions are then dragged downstream by an electron sheath created by the traveling magnetic field. It is worth mentioning that this effect is local and takes place on the magnetic field front. The ion velocity is initially close to the traveling magnetic field velocity as we can observe from the plots in $11\mu s$ (B) and $11.4\mu s$ (C).

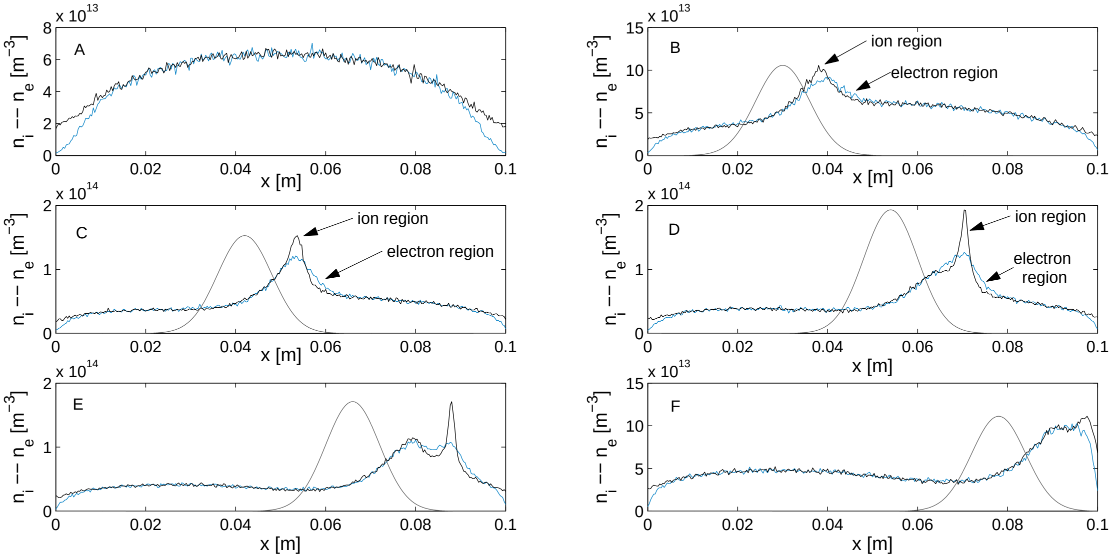

Figure 9. Ion (black) and electron (blue) densities at different time steps. A: $10\mu s$. **B:** $11\mu s$. **C:** $11.4\mu s$. **D:** $11.8\mu s$. **E:** $12.2\mu s$. **F:** $12.6\mu s$.

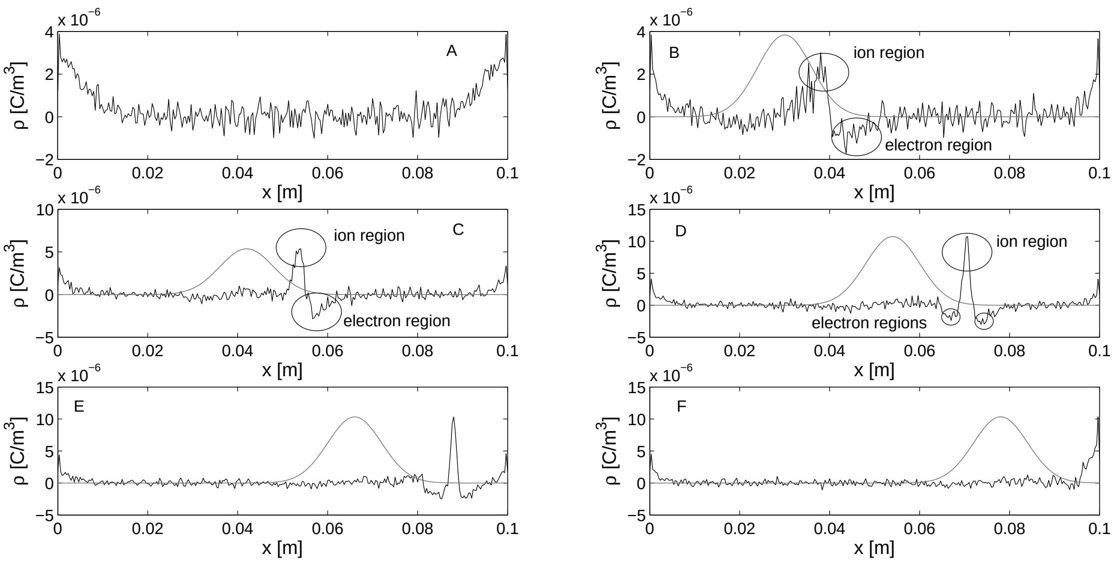

Figure 10. Charge density at different time steps. A: $10\mu s$. **B:** $11\mu s$. **C:** $11.4\mu s$. **D:** $11.8\mu s$. **E:** $12.2\mu s$. **F:** $12.6\mu s$.

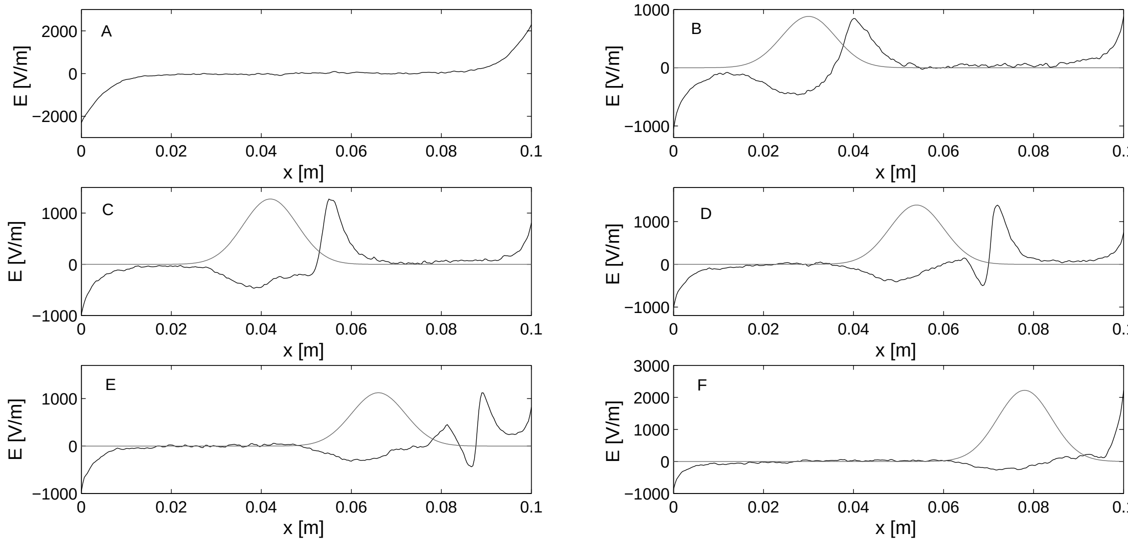

Figure 11. Electric field at different time steps. A: $10\mu s$**. B:** $11\mu s$**. C:** $11.4\mu s$**. D:** $11.8\mu s$**. E:** $12.2\mu s$**. F:** $12.6\mu s$**.**

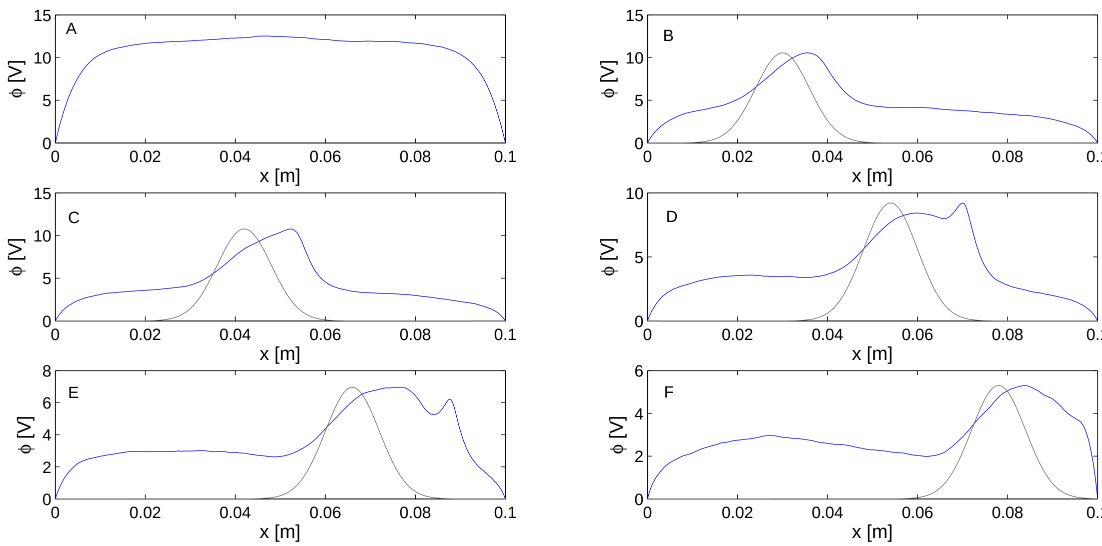

Figure 12. Electrostatic potential at different time steps. A: $10\mu s$**. B:** $11\mu s$**. C:** $11.4\mu s$**. D:** $11.8\mu s$**. E:** $12.2\mu s$**. F:** $12.6\mu s$**.**

During the propagation of the magnetic field through the plasma, the electrostatic structure formed at the magnetic front changes its characteristics. The positively charged region becomes surrounded by negatively-charged sheaths on both sides. A high velocity ion population forms and propagates downstream with a velocity higher than the traveling velocity of the magnetic field. The time evolution of the electrostatic structure is illustrated in Figure 13. The plot highlights the space propagation of the potential hill moving together with the magnetic field.

The simulations presented here, although performed with a 1D model with simplifying assumptions, point out a possible mechanism of plasma acceleration induced by a traveling magnetic field. The results show the fundamental role of electrons as carriers of the acceleration. A more complete picture requires additional simulations in order to explore different ion species, magnetic field strengths and velocities. Particularly, if the magnetic field is sufficiently high, even the ion motion can be directly affected by the magnetic pulse

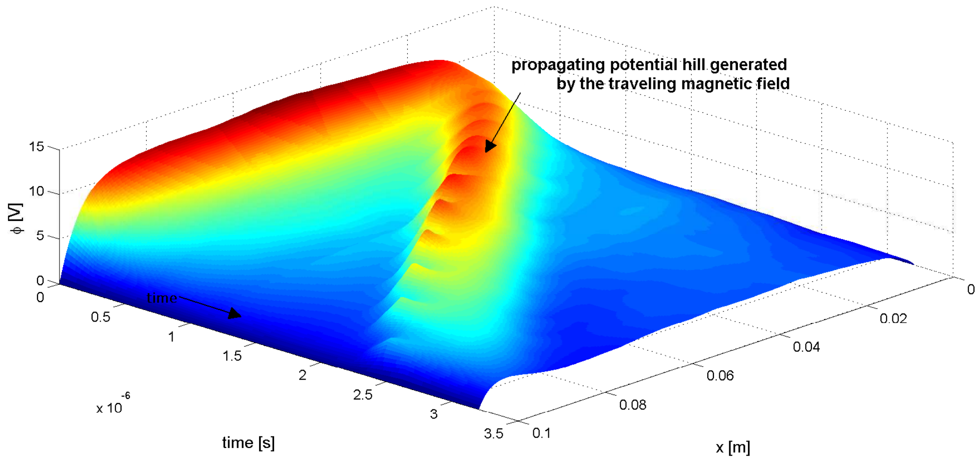

Figure 13. Time evolution of the potential along the simulation domain.

(since $\tau_{ic} < w/2v_t$), above all in case of light ions, creating a different physical frame.

IV. Experimental setup

We have designed and built an accelerator prototype based on a transmission line configuration. The accelerator is an array of ten coils connected in series and presents an inner diameter of $26mm$ and length of $110mm$. Each coil is made of 9 windings, arranged in 3 rows and 3 columns. The inductance of each coil as measured through an impedance meter is equal to $2.68\mu H$. The transmission line consists of $0.1\mu F$ capacitors connected in parallel, according to the scheme illustrated in Figure 2. The circuit is terminated by a 5Ω resistive load. The estimated propagating velocity of the traveling magnetic field using Eqn. 4 is about $21500m/s$. The circuit has been designed with the support of Matlab and Simulink models.

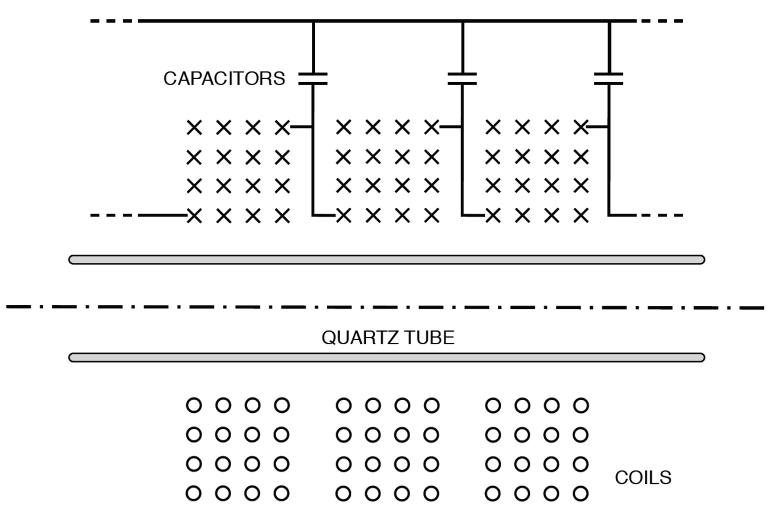

Figure 14. Schematic of the designed prototype.

A. Design for continuous mode operations

For continuous operation the transmission line is powered by a $280kHz$-$300W$ RF power supply. According to this frequency the current in each coil is phase shifted by about 50° relative to the previous coil. At a given time step, the currents in the coils shape a sinusoidal profile in space with a wavelength of $v_t/f = 75mm$. The system has been designed to have 1.5 spatial wavelengths along the accelerator length.

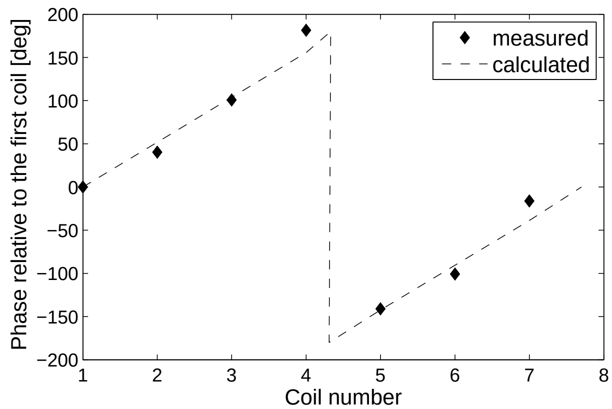

Figure 15. Predicted and measured phase shifts of the coils relative to the first one.

In order to verify the correct behavior of the transmission line we have measured the voltage at each connection between the coils and compared to the analytical predictions. The phase shifts relative to the first coil are plotted in Fig.15.

B. Design for pulsed mode operations

In the pulsed mode a $1\mu F$ capacitor is discharged generating a current pulse propagating along the transmission line. A hammer relay is used for connecting the capacitor to the transmission line. The applied voltage spans in the $1-2kV$ range giving pulse energies of $0.5-2J$. The current flowing through the first and last coil is measured using Pearson probes located at the beginning and at the end of the accelerator. The $7.5\mu s$ time delay between the two currents peak gives a propagation velocity of $15000m/s$.

C. Diagnostic systems and preliminary experiments

We are currently performing preliminary experiments to verify the effectiveness of the acceleration provided by the new system. The $2.45GHz$ Evanson microwave cavity used as the primary ionization stage is installed upstream of the accelerator and is operated continuously at $100W$. The quartz tube is mounted outside the vacuum chamber and connected to it through a flange. The pumping is provided by a cryogenic panel, leading to a background pressure of $5 \cdot 10^{-6}mbar$ and a pressure of $2-6 \cdot 10^{-5}mbar$ during the accelerator operation. A Pearson probe is used to monitor the current flowing through the coils. In order to detect the accelerated plasma sheet a time-of-flight probe has been built and installed downstream the accelerator. The probe is made of two copper conductors spaced $1.25cm$ apart (see Fig. 16). Only the end of the conductors is exposed to the plasma while the remaining part is encased in an alumina tube. A third conductor, completely insulated, has been introduced in order to determine the signal generated by possible electromagnetic interferences; this allows for the identification of the component of signal picked-up by the exposed conductors which is effectively produced by a propagating plasma sheet. Moreover time-varying magnetic field probes are available to measure the intensity of the traveling field. A photograph of the experimental facility while in operation is shown in Fig. 17.

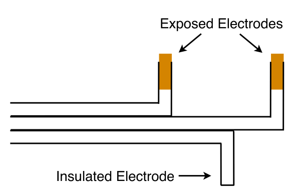

Figure 16. Scheme of the time-of-flight probe with two exposed electrodes and an insulated one.

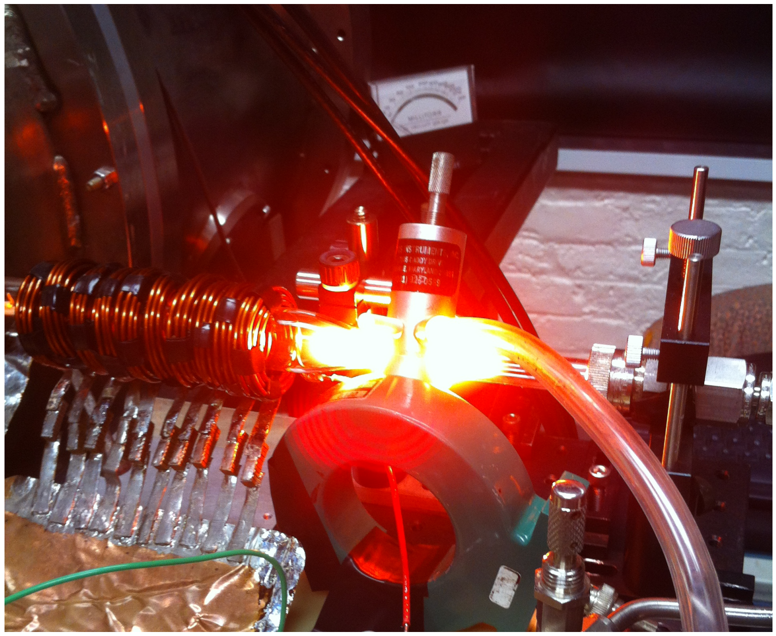

Figure 17. Photograph of the experimental arrangement with the coil system that generates the traveling magnetic field. The circuit is a transmission line. The plasma source which injects ions into the accelerator stage is an Evanson cavity operating at 2.45 GHz and about 100 W of power (neon feed).

V. Conclusions

The analysis performed through the particle-in-cell model highlights a possible acceleration mechanism induced by a magnetic pulse propagating in a uniform plasma. The field preferentially acts on electrons whereas its direct effect on ions is negligible for the field strengths employed. Due to the different dynamics of ions and electrons a charge separation forms at the magnetic front creating an electrostatic structure which accelerates ions. This structure propagates together with the wave. This concept can be exploited in a dual-stage propulsion system, where the neutral propellant flow is ionized by a high efficiency source (e.g. helicon) and then accelerated by a traveling magnetic field. Such a system can offer several possible advantages: it is electrodeless, can operate with different propellants and does not require an external neutralizer. A prototype of the accelerator has been designed and built using a microwave cavity for ionization and a transmission line circuit to generate the propagating magnetic field. An experiment has been set up in order to carry out preliminary experimental investigations.

Acknowledgments

ALF is grateful to the "Fondazione Aldo Gini" scholarship for supporting his stay at Stanford University in 2012, where this work was carried out.

References

[1]N. Gascon, M. Dudeck, S. Barral, "Wall Material Effects in Stationary Plasma Thrusters. Parametric studies of an SPT-100," *Physics of Plasmas*, Vol. 10, No. 10, 2003.

[2]O. Batischev, "Minihelicon Plasma Thruster," *IEEE Transactions on Plasma Science*, Vol. 37, No. 8, 2009.

[3]B.G. Gardineer IV, B. Jorns, and E.Y. Choueiri, "Simulations of Direct Ion Acceleration with Beating Electrostatic Waves," *32nd International Electric Propulsion Conference*, IEPC2011-212, Wiesbaden, Germany, 11-15 Sept. 2011.

[4]T.Nakamura, K.Yokoi et al., "Experimental Investigation of Plasma Acceleration by Rotating Electric

field for Electrodeless Plasma Thruster," *32nd International Electric Propulsion Conference*, IEPC2011-279, Wiesbaden, Germany, 11-15 Sept. 2011.

[5]R.H. Lovberg, C. L. Dailey, "Large Inductive Thruster Performance Measurement," *AIAA Journal*, Vol. 20, No. 7, 1982.

[6]E. Y. Choueiri, K. A. Polzin, "Faraday Acceleration with Radio-Frequency Assisted Discharge," *Journal of Propulsion and Power*, Vol. 22, No. 3, May-June 2006.

[7]C.W.Haldeman, J.P.Sullivan, E.Covert, "A Variable Phase Velocity Traveling Wave Pump," *AIAA Journal*, Vol. 9, No. 7, 1971.

[8]R.E. Jones, R.W. Palmer, "Traveling Wave Plasma Engine Program at NASA Lewis Research Center," *Third Annual Conference on Engineering Magnetohydrodynamics*, Rochester, NY, 28-29 March 1962.

[9]R.E. Jones, R.W. Palmer, "Experimental Investigation a Constant-Velocity Traveling Magnetic Wave Plasma Engine," *NASA Technical Note*, NASA TN D-2676, 1965.

[10]R.E. Jones, R.W. Palmer, G.R Seikel, "Analytical Investigation of Coils-System Design Parameters for a Constant-Velocity Traveling Magnetic Wave Plasma Engine," *NASA Technical Note*, NASA TN D-2278, 1964.

[11]C.G. Light, "Magnetic Insulation Experiments with a Traveling Magnetic Piston Plasma Accelerator," report prepared for Commander Space Systems Division US Airforce, Aerospace Corporation, El Segundo, California, 1963.

[12]G.R. Seemann, J.A. Thornton, A.S. Penfold, "Experimental Study of a Traveling Wave Accelerator," *AIAA Journal*, Vol. 4, No. 1, 1966.

[13]R.G. Jahn, "Physics of Electric propulsion," published by Dover Publications, 2006, pp. 306-313.

[14]L. Heflinger, S. Ridgway, A. Schaffer, "Transvere Traveling Wave Plasma Engine," *AIAA Journal*, Vol. 3, No. 6, 1965.

[15]A. Schaffer, "Plasma Propulsion with a Pulsed Transmission Line," *ARS Journal*, Vol. 31, No. 12, 1961.

[16]F. C. Fehsenfeld, K. M. Evenson, H. P. Broida, "Microwave Discharge Cavities Operating at 2450 MHz," *Rev. Sci. Instrum.*, Vol. 36, No. 3, 1965.

[17]A. Collodo supervised by D. Pavarin and A. Lucca Fabris, "Development of one-dimensional particle codes for the simulation of plasmas for aerospace propulsion," *Thesis for the degree of Aerospace Engineer*, University of Padova, 2011.

[18]A.J. Lichtenberg, M.J. Lieberman, "Principles of Plasma Discharges and Materials Processing," published by Wiley, 2nd edition, 2005.